Geophys. J. Int. (2005) **161,** 102–112 doi: 10.1111/j.1365-246X.2005.02564.x

Temperature dependence of magnetic susceptibility in an argon environment: implications for pedogenesis of Chinese loess/palaeosols

Qingsong Liu,[1,2] Chenglong Deng,[2] Yongjae Yu,[3] José Torrent,[4] Michael J. Jackson,[1] Subir K. Banerjee[1] and Rixiang Zhu[2]

[1] *Institute for Rock Magnetism, Department of Geology and Geophysics, University of Minnesota, Minneapolis, MN, USA. E-mail: liux0272@yahoo.com*
[2] *Paleomagnetism Laboratory, Institute of Geology and Geophysics, Chinese Academy of Sciences, Beijing, China*
[3] *Geosciences Research Division, Scripps Institution of Oceanography, La Jolla, CA, USA*
[4] *Departamento de Ciencias y Recursos Agrícolas y Forestales, Universidad de Córdoba, Apdo 3048,* 14080 *Córdoba, Spain*

Accepted 2004 December 15. Received 2004 November 27; in original form 2004 May 17

SUMMARY

Temperature dependence of magnetic susceptibility ($\chi - T$) has been widely used to determine changes in mineralogy of natural samples during heat treatment. We carried out integrated rock magnetic experiments to interpret the $\chi - T$ curves of the Chinese loess/palaeosols in argon. We used both raw materials and heated samples. In addition, we also investigated the magnetic properties of magnetic extracts and residues to quantify contributions from each fraction to the bulk magnetic properties. For the heating curves, the susceptibility loss (∼30 per cent) between ∼300–400 °C is caused by the inversion from pedogenic fine-grained maghemite to haematite, suggesting that the susceptibility loss can be used as a new concentration index of the pedogenic fine-grained superparamagnetic (SP) particles in the Chinese loess/palaeosols. Unlike the warming curves, the cooling curves are dominated by newly formed fine-grained magnetites with a dominant size of ∼35 nm. The onset for the new production of these fine-grained magnetic particles occurs at ∼400 °C. It is interesting that the room-temperature magnetic susceptibility (χ_{ph}) of the samples heated after a 700 °C run is independent of the degree of pedogenesis and saturates at approximately 33–35 $\times$ 10^{-7} m^3 kg^{-1}, indicating that the susceptibility enhancement is controlled only by the reduction of Fe-bearing aeolian minerals during heating. It appears that the 700 °C thermal treatment in argon could be in some sense an analogue to the pedogenic processes. Thus, we predict that ∼33–35 $\times$ 10^{-7} m^3 kg^{-1} is the maximum susceptibility that pedogenesis can generate for the last interglacial palaeosol unit (S1). In practice, χ_{ph} would be useful to quantify the aeolian inputs to the Chinese Loess plateau.

Key words: Chinese loess/palaeosols, pedogenesis, temperature dependence of magnetic susceptibility, Yuanbao.

1 INTRODUCTION

Temperature dependence of magnetic susceptibility (hereafter referred to as $\chi - T$), specifically the stepwise $\chi - T$ measurement (or partial heating/cooling cycles; Mullender *et al.* 1993; van Velzen & Dekkers 1999; Deng *et al.* 2000, 2001; Hrouda 2003; Hrouda *et al.* 2003; Zhu *et al.* 2003; Deng *et al.* 2004; Zhu *et al.* 2004), is sensitive to subtle changes in magnetic minerals during thermal treatments and has been used as a routine rock magnetic tool to identify the magnetic mineralogy.

Compared with temperature dependence of saturation magnetization (M_s; referred to as $M_s - T$), $\chi - T$ curves are more strongly controlled both by magnetic mineralogy and by grain size distributions. Therefore, $M_s - T$ measurements are generally preferred in determining the Curie temperature (T_C). However, once the physical mechanism behind the $\chi - T$ curves for certain samples is understood, $\chi - T$ curves may have broader applications (e.g. indications for grain sizes).

$\chi - T$ has been widely used in the Chinese loess/palaeosol studies because it can further indicate the degree of pedogenesis of the loess/palaeosols (e.g. Deng *et al.* 2001, 2004). The Chinese Loess plateau is located in the eastern Asian monsoon zone. The low-field magnetic susceptibility of samples is carried both by aeolian coarse-grained magnetic inputs and by pedogenically produced fine-grained magnetic particles (Maher & Thompson 1991, 1992; Verosub *et al.* 1993; Fine *et al.* 1995; Heller & Evans 1995). In general, during

 © 2005 RAS

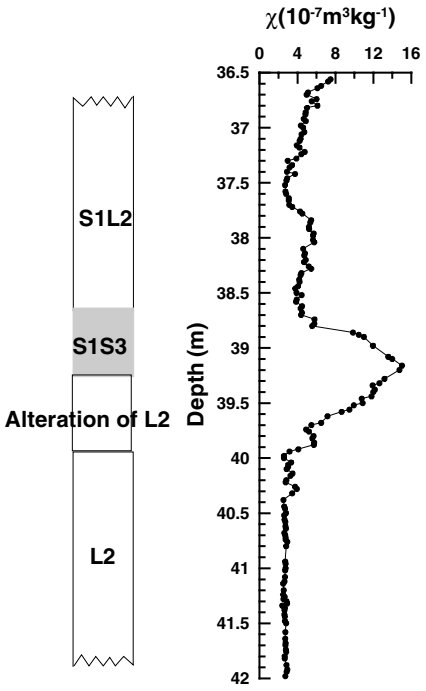

Figure 1. Stratigraphy and susceptibility of the YB profile (Liu *et al.* 2004a).

cold/dry periods, the winter monsoons bring sediments from northern and northwestern sources (Liu 1985; Sun 2002), and deposit them at the Loess plateau with minor pedogenic alterations. In contrast, during warm/humid periods, aeolian inputs decrease and soils begin to develop. The neoformation of the extremely fine-grained superparamagnetic (SP) grains significantly enhances the susceptibility of palaeosols (Zhou *et al.* 1990; e.g. shown in Fig. 1). Thus, the palaeoclimatic variations are manifested by the changes of the magnetic mineralogy and grain size of the loess/palaeosols, and can be recognized by $\chi - T$ measurements (Deng *et al.* 2000, 2001, 2004).

Previous measurements have documented that the major $\chi - T$ behaviour of the Chinese loess/palaeosols is predictable (e.g. characteristic curves in Fig. 2; Florindo *et al.* 1999; Deng *et al.* 2000, 2001; Zhu *et al.* 2003; Deng *et al.* 2004). For example, the warming curve shows two peaks at ∼300 and 500–550 °C, respectively (Fig. 2a). T_C of ∼580 °C demonstrates the presence of nearly stoichiometric magnetite (Fig. 2a). However, whether the stoichiometric magnetite is originally present in the samples or formed during heating needs further clarification. The gradual decrease of susceptibility between ∼300–450 °C (Fig. 2a) has been attributed to the inversion from strongly magnetic but thermally unstable maghemite to weakly magnetic haematite (Sun *et al.* 1995; Oches & Banerjee 1996; Florindo *et al.* 1999; Zhu *et al.* 1999; Deng *et al.* 2000, 2001; Zhu *et al.* 2003; Deng *et al.* 2004). In contrast, the cooling curve simply shows a single peak at ∼400 °C (Fig. 2b).

Despite these intensive investigations, mineral transformations during heating/cooling processes have not been completely settled. The main reason is that all the previous studies simplified the interpretation by focusing on the chemical variation and neglecting physical aspects such as grain size variations. In order to incorporate the effect of grain size variations on $\chi - T$, we physically extracted the magnetic minerals from the matrix, and then measured the $\chi - T$ curves separately both for bulk samples and for the extracted fractions. By combining various rock magnetic measurements, we aimed to determine variations in both magnetic mineralogy and grain sizes during laboratory heating. Finally, the pedogenic implications of the $\chi - T$ curves will be further specified.

2 SAMPLING AND EXPERIMENTS

2.1 Samples

The Yuanbao (YB) section (35°38′N, 103°10′E) is located in the northwestern margin of the Chinese Loess plateau on the fourth terrace of the Daxia river in the Linxia basin. Stratigraphy of this profile has been previously established (Chen *et al.* 1999; Liu *et al.* 2004a). The ∼8-m palaeosol unit S1 (MIS 5) consists of three well-developed subpalaeosol units (S1S1, S1S2 and S1S3) and two interbedded subloess layers (S1L1 and S1L2). For this profile, we focus on the sandwich sequence S1L2/S1S3/L2 spanning a complete climatic cold/warm/cold cycle (Fig. 1).

To quantify the contributions of the magnetic fraction (ferrimagnetic and antiferromagnetic minerals) and non-magnetic matrix fraction (paramagnetic and diamagnetic minerals) to the bulk

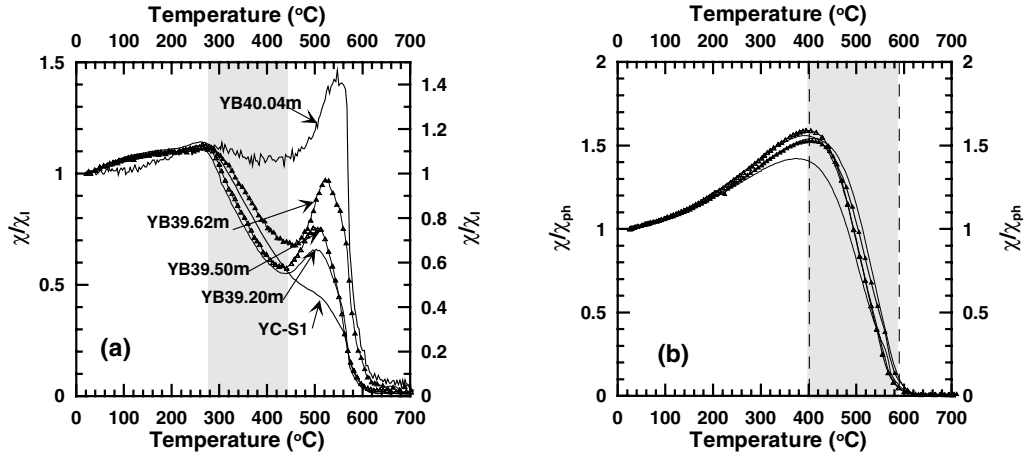

Figure 2. (a) Warming and (b) cooling runs of χ curves for the five selected samples. Grey bars in (a) and (b) highlight a gradual decrease of susceptibility between 300 and 450 °C during warming and a gradual increase between 400–600 °C during cooling, respectively. YC-S1 is the most mature palaeosol sample collected from the Yichuan section (Liu *et al.* 2002) and is used as an end-member of palaeosol samples for comparison.

properties, magnetic extracts of the palaeosol sample at 39.2 m and the loess sample at 40.04 m were obtained in a continuous-loop flow driven by a pump, using a high-gradient magnet. Each separation lasted approximately two weeks to sufficiently extract the magnetic minerals from samples. Systematic rock magnetic experiments were conducted on bulk samples, residues and magnetic extracts.

2.2 Experiments

The low-field mass-specific magnetic susceptibility (χ) was measured using a Kappa bridge (KLY-2). The $\chi - T$ curves above the room temperature were also measured using the Kappa bridge equipped with a CS-2 furnace from room temperature to 700 °C in an argon environment (the flow rate is 100 ml min^{-1}). Before the thermal treatments, air in the holder was flushed out to avoid the effects of oxygen during heating. The maximum treatment temperature is 700 °C with a step of 5 °C. Each run started with raw loess/palaeosol of ∼300 mg and took approximately 3 hr. The average heating and cooling rates are approximately 7.5 °C min^{-1}. The 700 °C heat-treated samples exhibit a homogeneously black colour, indicating uniform alterations of samples. The low-temperature $\chi - T$ curve for the loess sample at 40.04 m was measured using a Quantum Design SQUID magnetometer (MPMS).

Hysteresis loops were measured at room temperature using a Princeton Measurements Corporation vibrating sample magnetometer (MicroMag 3900), with a maximum applied field of 1 T, after heating in temperature increments of 50 °C. Saturation magnetization (M_s), saturation remanence (M_{rs}) and coercivity (B_c) were obtained after subtracting the paramagnetic contribution (high-field slope).

Frequency dependence of magnetic susceptibility was measured using a Lake Shore Cryotronics AC Susceptometer for the sample at 39.5 m and the corresponding thermal products to detect the possible changes in SP grains during heating. Absolute frequency dependence of susceptibility $\chi_{fd}(\chi_{400\,Hz} - \chi_{4000\,Hz})$ was calculated by least-squares with data (20 points) acquired between 400 and 4000 Hz at room temperature.

Anhysteretic remanent magnetization (ARM) was imparted in a 200 mT alternating field with a superimposed 50 μT direct bias field using a Dtech D2000 instrument. ARM was then normalized by the bias field to obtain ARM susceptibility (χ_{ARM}). The χ/χ_{ARM} ratio (dimensionless) is used to investigate relative contributions of SP and single domain (SD) grains to the bulk signal.

3 RESULTS

3.1 $\chi - T$ measurements

Typical $\chi - T$ curves are shown in Fig. 2. There are two major peaks occurring around 280 and 510 °C for the warming curves (Fig. 2a). The gradual decrease in χ between 300 and 440 °C (light grey zone) is almost absent for the loess sample (40.04 m). With increasing pedogenesis, this susceptibility loss increases (Fig. 2a). In contrast, the cooling curves for all the samples show a dominant peak at ∼400 °C (Fig. 2b).

To quantify contributions of the magnetic extracts and residues to bulk samples, $\chi - T$ curves for the extracts of the loess and palaeosol samples are presented in Figs 3 and 4, respectively. In Figs 3(a), (b), 4(a) and (b), the values are normalized by initial room-temperature susceptibility of the bulk sample. In contrast, in Figs 3(c), (d), 4(c) and (d), the susceptibility curves are normalized by the initial χ_I of the individual fractions.

For the loess, we observed nearly replicated patterns of the warming curves for the bulk sample and the magnetic extracts, suggesting that the bulk information is dominated by the extractable coarser-grained ferrimagnetic particles (Fig. 3a). The post-heating room temperature susceptibility of the 700 °C–treated samples is denoted as χ_{ph}. For cooling curves, the sum of χ_{ph} for residue and extractable magnetic material is only one-third that of the bulk sample. Unlike the loess sample, the warming curve of the palaeosol bulk sample is determined by the non-extractable finer grained ferrimagnetic material in residue (Fig. 4a) and the extractable portion has only a minor contribution.

Another notable feature of the palaeosol sample is the change in the temperatures ($T_{\chi-max}$) at which the maximum susceptibility occurs. $T_{\chi-max}$ has been well studied (Gittleman *et al.* 1974; Khater *et al.* 1987; Chantrell *et al.* 1991). It is directly related to the mean blocking temperature (T_B) of the system and in turn the product of the microcoercivity (H_k) and volume (V) of particles. Assuming a constant distribution of microcoercivity, there is a relationship between the grain size (or volume) and $T_{\chi-max}$ (Liu *et al.* 2004b). In general, a lower $T_{\chi-max}$ corresponds to a finer grain size. $T_{\chi-max}$ values for the extractable portion, bulk sample and residues for the palaeosol sample at 39.5 m are 440, 410 and 385 °C, respectively (Fig. 4d). Fig. 5 compares the thermal behaviour of the magnetic extracts for the loess and palaeosol samples. We also found that the $T_{\chi-max}$ on warming of the loess extract is approximately 520 °C, which is approximately 40 °C higher than that of the palaeosol extract.

Systematic changes in partial warming/cooling cycles for the palaeosol sample at 39.5 m are shown in Figs 6(a) and (c). Fig. 6(c) is a magnification of the high temperature part of Fig. 6(a). The ratio of χ_{ph}/χ_I and the corresponding normalized $M_s(M_s/M_{s0}$; M_{s0} is the M_s of the raw material) are summarized in Figs 6(b) and (d). Changes in M_s and χ are not in phase at all temperature intervals, indicating that the magnetic carriers for these two magnetic parameters are different. With increasing treatment temperature T_{tr}(< 280° C), both χ_{ph}/χ_I and M_s/M_{s0} slightly increase. Between 280 and 430 °C, susceptibility decreases by approximately 30 per cent, but M_s remains relatively stable. Above 430 °C, these two parameters sharply increase but with different rates. For example, at T_{tr} = 600° C, M_s is approximately 12 times higher than M_{s0}, but the corresponding χ_F is only enhanced by ∼300 per cent, resulting in gradual decreases in the ratio of χ_F/M_s with increasing T_{tr}.

$T_{\chi-max}$ on cooling systematically decreases with increasing T_{tr} (Figs 6a and c), indicating that the neoformed magnetic particles become finer and finer when increasing T_{tr}. Fig. 7 plots the ratio χ_{ph}/χ_I against χ of all the samples examined in this study. With increasing χ_I, χ_{ph}/χ_I decreases. However, χ_{ph} is nearly susceptibility independent, with a constant value around 33×10^{-7} m^3 kg^{-1} (Fig. 7b).

3.2 Magnetic hysteresis

Room temperature hysteresis properties of the intermediate thermal products of the 39.5-m palaeosol sample are shown in Fig. 8. When T_{tr} = 600 °C, B_c (Fig. 8a), B_{cr} (Fig. 8b), M_{rs} (Fig. 8c) and M_s (Fig. 8d) have increased by factors of ∼2.7, ∼2.0, ∼18.7 and 10.6, respectively. Below 400 °C, the decrease of M_{rs}/M_s (Fig. 8e) and the corresponding increase of B_{cr}/B_c (Fig. 8f) suggest that the average grain size of the magnetic minerals in the sample becomes

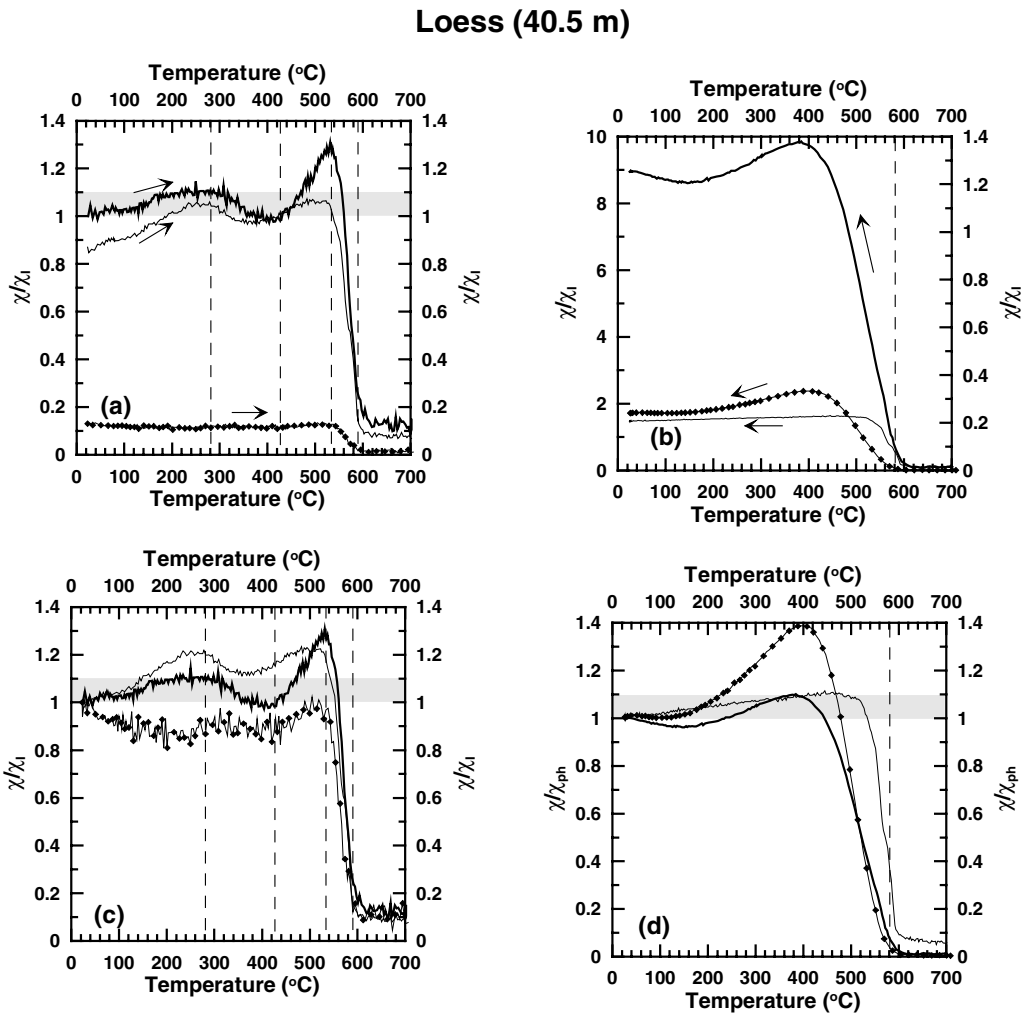

Figure 3. Warming (a, c) and cooling runs (b, d) of $\chi - T$ curves for the loess sample at 40.04 m. The curves in (a) and (b) are normalized by the initial susceptibility of the raw loess sample to quantify the relative contribution of the residue (diamonds) and magnetic extracts (thin lines) to the bulk information (thick lines) during the warming/cooling cycles. In (c) and (d), curves are normalized by its susceptibility at 25 °C, respectively.

coarser. In contrast, the abrupt changes in these two ratios above 400 °C indicate that the bulk magnetic properties of the sample are dominated by the newly formed magnetite. During heating, the high-field slope (resulting from paramagnetic and antiferromagnetic material; Fig. 8g) also increases slightly below ∼500 °C and sharply above ∼500 °C, respectively. Fig. 8(h) shows systematic changes in the average magnetic grain sizes with T_{tr}. Clearly, between 280–375 °C, the grain size increases and, above 375 °C, it decreases. The endpoint M_{rs}/M_s at 600 °C is ∼0.29.

3.3 Frequency and temperature dependence of magnetic susceptibility

Frequency dependence of magnetic susceptibility is very sensitive to SP particles with size around 20 nm (Maher 1988). Susceptibility slightly decreases with increasing frequency, indicating the existence of SP particles. To quantify the absolute changes in SP concentrations, $\chi_{fd}(\chi_{400\,Hz} - \chi_{4000\,Hz})$ versus T_{tr} is plotted for a sample at 39.50 m in Fig. 9(b). From 150 to 280 °C (where a maximum χ is observed on the $\chi - T$ warming curve, Fig. 2a), χ_{fd} slightly increases, but the relative χ_{fd} per cent decreases. Above 280° C, χ_{fd} begins a gradual 30 per cent decrease from 0.80×10^{-7} m^3 kg^{-1} at 150 °C to 0.55×10^{-7} m^3 kg^{-1} at 400 °C. Above 500° C, χ_{fd} sharply increases to 1.98×10^{-7} m^3 kg^{-1} at 600 °C, indicating that two different processes occur below and above 500 °C. Fig. 9(c) shows the relative contribution of SP grains to the bulk sample. Even though the 600 °C thermal product has an absolute χ_{fd} more than twice that of the 150 °C thermal product, the corresponding relative χ_{fd} per cent of the former is approximately 2 per cent lower than that of the latter, strongly suggesting that the susceptibility enhancement after the 500 °C treatment is not determined by SP grains. Fig. 9(d) shows the positive linear correlation ($R^2 = 0.95$) between the variations in SP concentrations, presented by χ_{fd}, and χ_{ph} for the thermal products, indicating that the changes in χ_F are highly related to the changes in SP concentrations during heating.

3.4 ARM

ARM and the corresponding interparametric ratio (χ/χ_{ARM}) against T_{tr} are shown in Fig. 10. ARM values steadily increase when $T_{tr} <$ 300 °C and decrease above (Fig. 10a). A second sharp increase in ARM occurs when $T_{tr} >$ ∼520 °C. The χ/χ_{ARM} ratio exhibits a U shape with increasing T_{tr} (Fig. 10b).

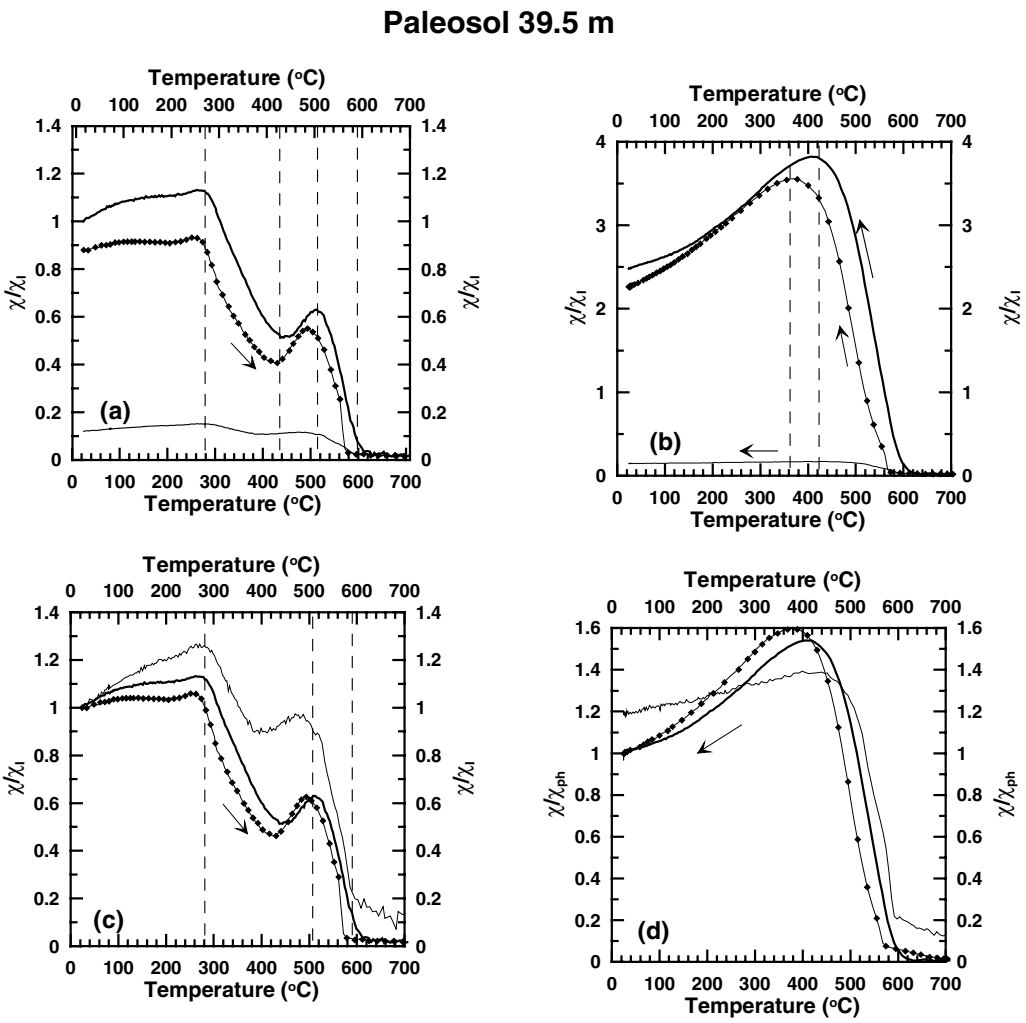

Figure 4. Warming (a, c) and cooling runs (b, d) of $\chi - T$ curves for the palaeosol sample at 39.20 m. The curves (a) and (b) are normalized by the initial susceptibility of the raw loess sample to quantify the relative contribution of the residue (diamonds) and magnetic extracts (thin lines) to the bulk information (thick lines) during the warming/cooling cycles. In (c) and (d), curves are normalized by its susceptibility at 25 °C, respectively.

4 DISCUSSION

4.1 Interpretation of the warming and cooling curves

For the warming curves, the gradual increase of susceptibility below ∼280 °C is the result of the gradual unblocking of fine-grained SD particles, which are SD at room temperature but become unlocked at elevated temperatures. The susceptibility drop between ∼300–400 °C has been interpreted as the inversion from maghemite to haematite (Sun *et al.* 1995; Oches & Banerjee 1996; Florindo *et al.* 1999). Fig. 8(d) shows that M_s slightly decreases between 320 and 370 °C, partially supporting this inversion. This further indicates that the maghemite particles contribute more to the magnetic susceptibility than to M_s, and they are in the very fine grain size region (SP + SD). Variations in χ_{fd} (concentration proxy for SP grains) and χ_{ph} after heating the palaeosol sample at 39.5 m are positively correlated (Fig. 9d). Fig. 10(b) demonstrates that the gradual decrease in χ/χ_{ARM} is caused by a decrease in contributions of SP grains. In addition, the susceptibility loss (Fig. 2a) is gradually enhanced from loess to palaeosols, further supporting that alteration of pedogenic products of only fine-grained SP grains is the main factor controlling the thermal behaviour between 300–400 °C.

Özdemir (1990) reported that the transformation of synthetic SD maghemite to haematite takes place at 725 °C. de Boer & Dekkers (1996) also found the majority of the inversion of PSD and MD maghemite to haematite occurs at the higher temperatures above the 600 °C run and is not fully complete even after the 800 °C run. By directly investigating the natural PSD maghemite particles separated from a palaeosol sample, Liu *et al.* (2003) showed that thermomagnetic curves for a loess sample are reversible at least up to 455 °C, indicating that the coarse-grained maghemite of aeolian origin in the Chinese loess are fairly thermally stable. Their results revealed that the main inversion from maghemite to haematite defined by sharp drops in χ_{ph} starts at ∼550 °C. For the fine maghemite grains, some X-ray work revealed that they do convert rapidly to haematite (Gallagher *et al.* 1968), whereas some torque measurements indicate the opposite (Senno *et al.* 1967). It has been suggested that the degree of crystallographic perfection may be the most important factor determining the speed as well as temperature for conversion (Gallagher *et al.* 1968). Nevertheless, we can conclude that finer-grained maghemite has a lower inversion temperature than the coarser-grained particles.

In the present study, only the fine-grained pedogenic particles can be efficiently inverted to haematite between 300–400 °C

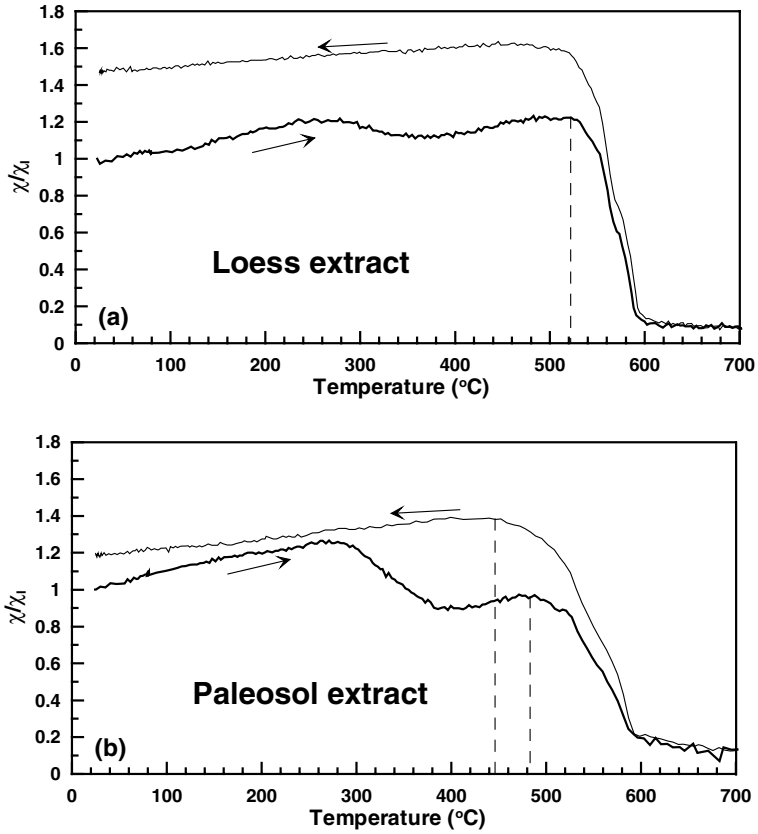

Figure 5. $\chi - T$ curves for the magnetic extracts from the loess sample (40.04 m; a) and the palaeosol sample (39.3 m; b). Arrows highlight the temperatures (T_{max}) corresponding to the maximum susceptibility. Clearly, on both the warming and cooling curves, the palaeosol extract has a lower T_{max} than the loess extract. In addition, the cooling curves are characterized as a lower T_{max} than the corresponding warming curves.

during heating. Thus, the susceptibility loss between 300–400 °C can be a proxy for quantifying the contributions of fine-grained pedogenic particles and, in turn, the degree of pedogenesis. If so, for general application, the susceptibility loss is superior to conventional χ_{fd} because it represents the contributions of all SP particles. Note that χ_{fd} is sensitive only to a small fraction of SP grains with grain size around 20–22 nm for maghemite. However, for the Chinese loess, these two SP indicators may be equivalent because the grain size distribution of pedogenic particles is nearly constant (Liu *et al.* 2004d). As a result, these two proxies are positively correlated.

Based on this model, approximately 30 per cent loss of magnetic susceptibility for palaeosols indicates that susceptibility carried by viscous SP particles is only ∼30 per cent of the bulk susceptibility. This is consistent with our recent independent estimation from the ARM measurements (Liu *et al.* 2004c), which show that pedogenically produced SD magnetic particles contribute more to the bulk susceptibility than SP particles because of a dense volume concentration of SD particles.

The grain sizes of the newly formed magnetite can be estimated by the temperature dependence of magnetic susceptibility. $T_{\chi-max}$ of ∼400 °C (Fig. 11) is an unblocking temperature of the newly formed magnetite particles in the thermal products. The corresponding estimated grain size is approximately ∼35 nm (Liu *et al.* 2004b). Thus, the continuous grain size distribution of the newly formed magnetite spans the SP and SD size region and reaches a maximum at ∼35 nm.

4.2 Pedogenic implication of χ_{ph}

The neoformed fine-grained magnetic particles in thermal products for both loess and palaeosols exhibit identical cooling behaviour, with a maximum susceptibility around 400 °C (Fig. 2b). This strongly indicates that the average grain size of these finer magnetite grains is pedogenesis independent. Moreover, the absolute value of χ_{ph}, which saturates at ∼33–35 × 10^{-7} m^3 kg^{-1} is also unrelated to pedogenesis (Fig. 7b). We therefore expect that χ_{ph} could relate solely to the aeolian inputs.

During the last several decades, many susceptibility measurements for loess/palaeosols of the Chinese Loess plateau have been made. The lowest loess susceptibility values are observed at the south margin of the Mu Us desert. From there, values increase exponentially southwards and eastwards by a factor of ∼7 at the northern front of the Qinling mountains (Porter *et al.* 2001), the traditional dividing line between north and south China. The maximum effects of pedogenesis are therefore expected to be observed at Xi'an, at the south margin of the loess plateau. Assuming that the source region and the general transport path of the dust have not significantly changed through time (Porter *et al.* 2001), the regional variations in S1 susceptibility will likely parallel the surface susceptibility. Thus, the maximum susceptibility estimated at Xi'an will be ∼34.7 × 10^{-7} m^3 kg^{-1}, which is consistent with the observed value ∼35 × 10^{-7} m^3 kg^{-1} at Xi'an by Eyre & Shaw (1994) and also consistent with the predicted χ_{ph}(33–35 × 10^{-7} m^3 kg^{-1}) in this study.

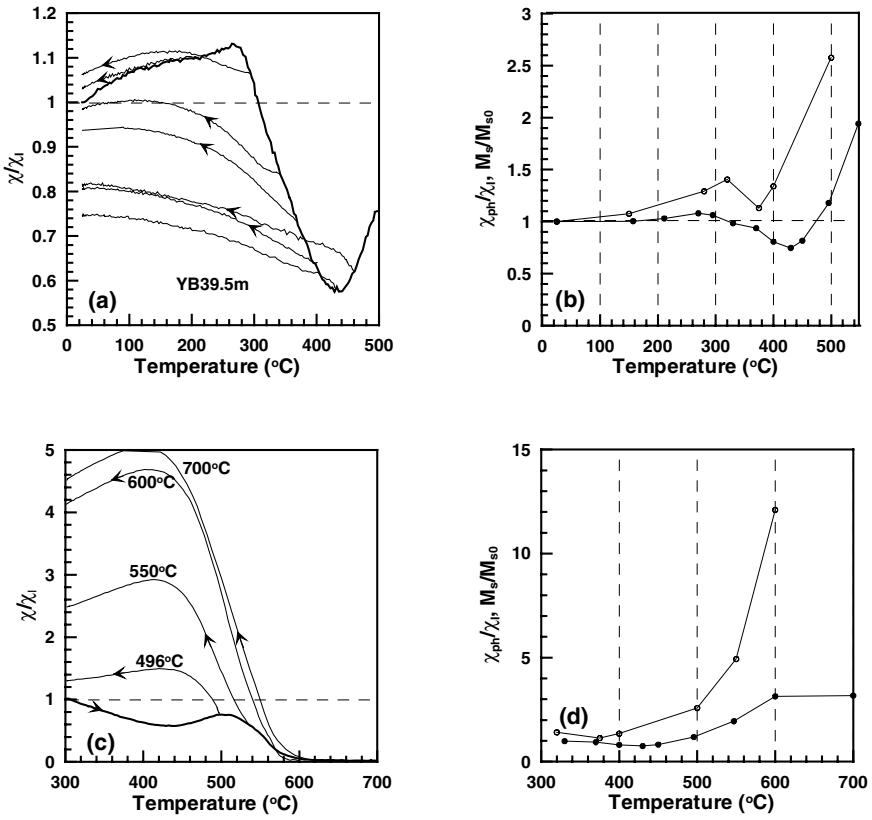

Figure 6. Partial $\chi - T$ curves for the palaeosol sample 39.5 m heated to different temperatures (a) and (c). Arrows indicate the warming and cooling processes. (b, d) χ_{ph}/χ_I (solid circles) and M_s/M_{s0} (open circles) against T_{tr}. M_{s0} is the initial M_s for the raw material.

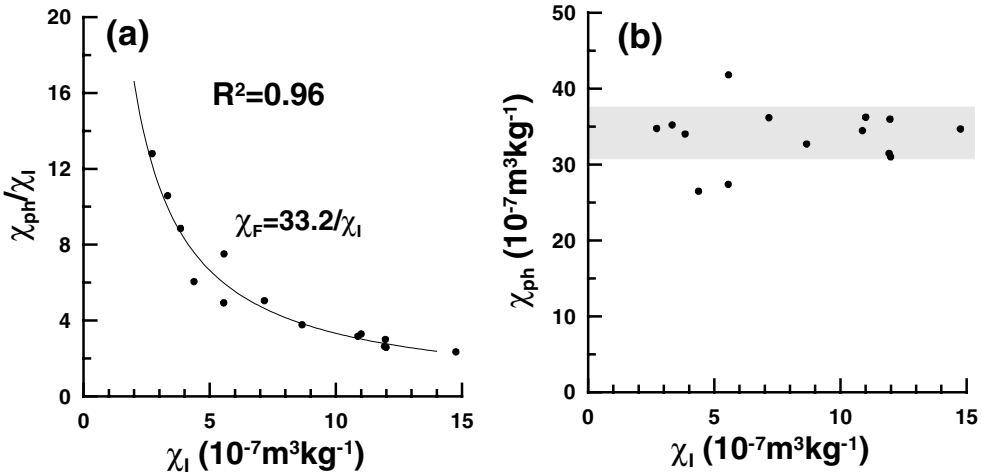

Figure 7. (a) Variations in χ_{ph}/χ_I versus χ_I. The line is the fitted trend with R^2 of 0.96. (b) χ_{ph} against χ_I.

The effects of pedogenesis and thermal treatment on the bulk susceptibility seem to be equivalent in this sense. Approximately 33–35 $\times$ 10^{-7} m^3 kg^{-1} is the maximum susceptibility that both pedogenesis and thermal effects can yield. The linkage of the effects of pedogenesis and the heating process has been discussed by Tite (1975). The χ_I of a worldwide soils varies significantly. However, the corresponding χ_{ph} values are very consistent, especially for the subset of limestone samples (Tite 1975).

The susceptibility enhancement of soils, i.e. the formation of ferrimagnetic minerals (magnetite and maghemite), is the result of several mechanisms, which include:

(1) bacterial production of magnetite in a reducing environment (as a result of the decay of organic matter in anaerobic conditions when the soil is wet);

(2) formation of magnetite in a reducing environment caused by the burning of organic matter;

(3) dehydroxylation of lepidocrocite to maghemite; and

(4) slow transformation of ferrihydrite to maghemite (Barrón & Torrent 2002 and references therein).

In the pedogenesis of Chinese loess, the iron that is released by the weathering of primary Fe-bearing silicates can be partly

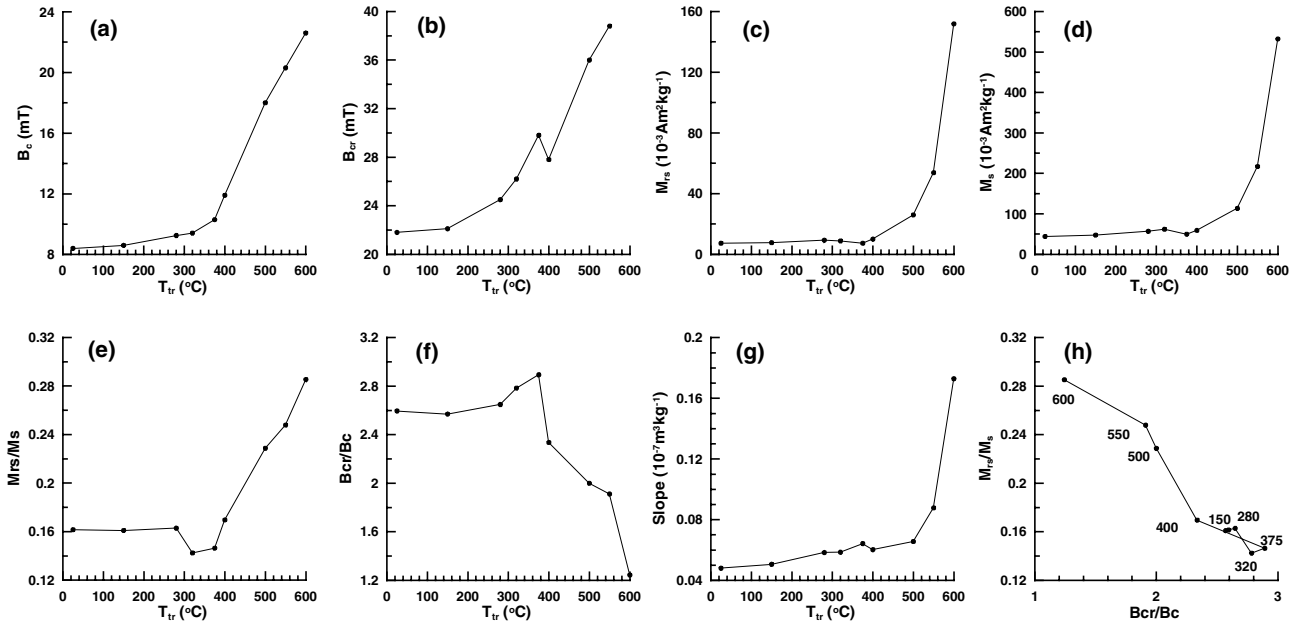

Figure 8. Hysteresis parameters of thermal products of the palaeosols sample (39.5 m). (a–g), B_c, B_{cr}, M_{rs}, M_s, M_{rs}/M_s, B_{cr}/B_c, high-field slope against the treatment temperature (T_{tr}), respectively. (h) Ratio of M_{rs}/M_s against B_{cr}/B_c named a Day plot (Day *et al.* 1977). Numbers in (h) are T_{tr}.

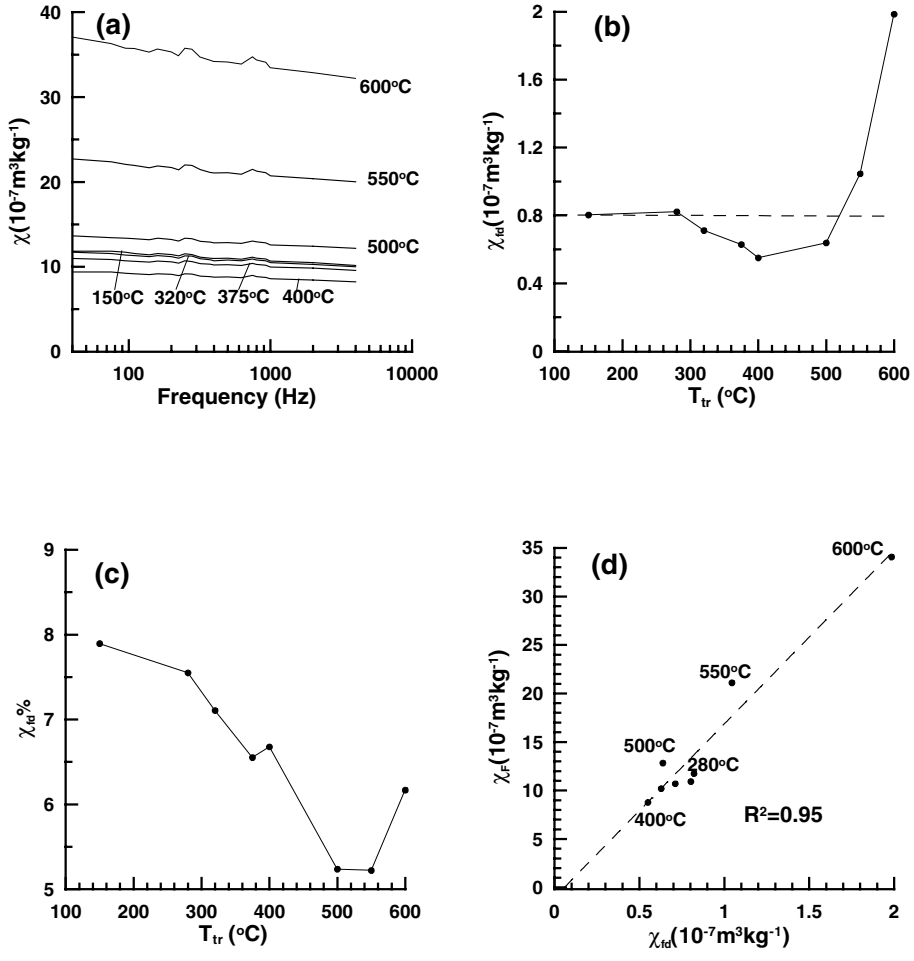

Figure 9. (a) Frequency-dependent susceptibility for the thermal products of sample YB39.50 m; (b) $\chi_{fd}(\chi_{400\,Hz} - \chi_{4000\,Hz})$ against T_{tr}; (c) χ_{fd} per cent against T_{tr}; (d) correlation between χ_{ph} and χ_{fd} for the thermal products. Dashed line in (d) is the linear trend with R^2 of 0.95.

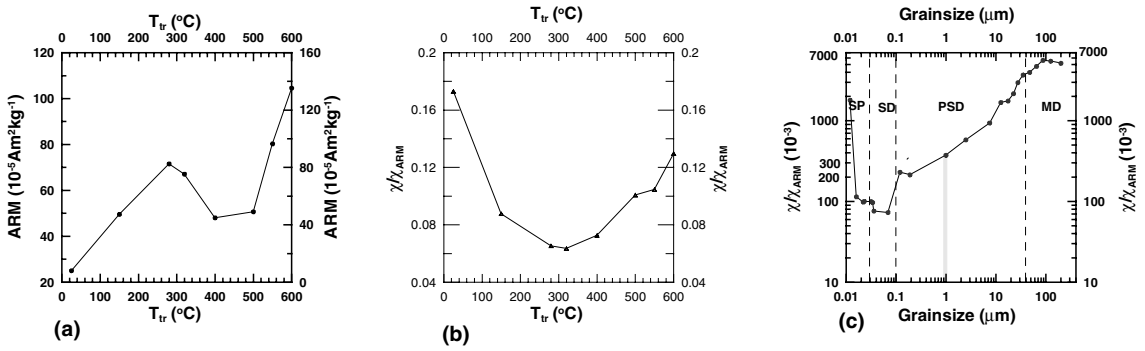

Figure 10. ARM (a) and χ/χ_{ARM} (b) against T_{tr}. Synthetic results of χ/χ_{ARM} versus grain size is shown in (c). Data in (c) are from the PhD thesis of Dankers (1978; $d > 1$ μm), Özdemir & Banerjee (1982; 70 nm $< d <$ 11 μm) and Maher (1988; $d <$ 70 nm).

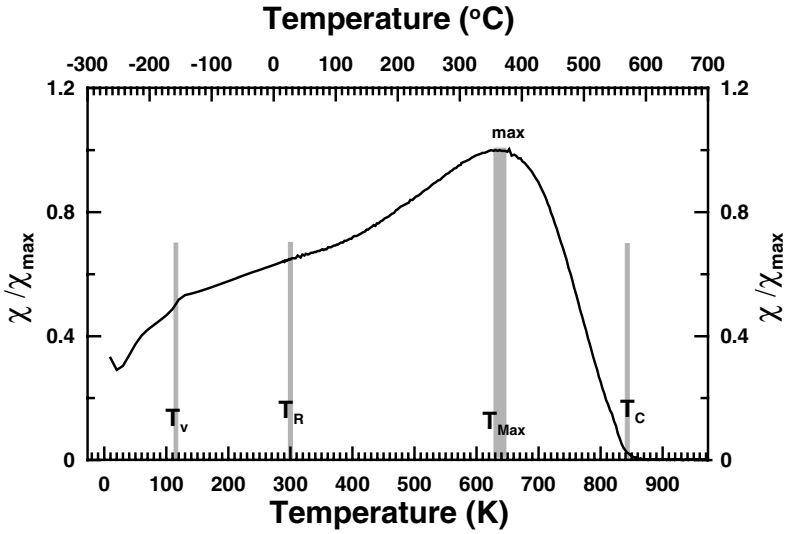

Figure 11. Temperature dependency of susceptibility between −253 °C (20 K) and 700 °C (973 K). T_{V}, T_{R} and T_{C} represent the Verwey transition (Verwey *et al.* 1947), room temperature and Curie temperature, respectively.

incorporated as Fe^{3+} or Fe^{2+} into a ferrimagnetic iron oxide via different mechanisms (Maher 1998). However, it must be recalled that the pedogenic alteration of Fe-bearing silicates results mostly in the production of goethite and haematite. So, the Chinese loess and palaeosols contain substantial amounts of goethite and haematite, both inherited and of pedogenic origin (Vidic *et al.* 2000; Ji *et al.* 2002; Deng *et al.* 2004; Ji *et al.* 2004). The haematite/goethite ratio depends on palaeoclimate and soil chemical environment. In particular, high temperatures and dry spells during the year favour haematite over goethite (Schwertmann & Taylor 1989).

During pedogenesis on loess, plant debris and iron-reducing bacteria may play a key role in formation of ultrafine magnetite. Because of the small size of many of the precipitated crystals, surface oxidation of magnetite to haematite or maghemite is likely to occur. Conversely, in a reducing environment, haematite can also be transformed into magnetite (Maher 1998). The pedogenic fine-grained magnetite is then a second-step alteration product.

Although some of the heating processes in the laboratory described above are different to the pedogenesis occurring in nature, there exists a similarity in two aspects. First, the pedogenesis occurs in a reducing environment. Secondly, the pedogenesis produces a fine-grained assemblage (SP + SD).

If the neoformation of SP + SD magnetites results from the reduction of haematite, then we would expect a much higher χ_{ph} for the palaeosols than for the loess samples because the former contain more pedogenic haematite particles. Therefore, pedogenic fine-grained haematite particles do not seem to be reduced to magnetite during heating. Otherwise, the fine-grained magnetite particles inverted from pedogenic haematite will significantly enhance χ_{ph}.

Because of the independence of χ_{ph} on the degree of pedogenesis, we conclude that the saturation of χ_{ph} is the result of the formation of ferrimagnetic minerals from Fe releaby the weathering or thermal alteration of Fe-bearing minerals in the loess (i.e. the so-called detrital or aeolian Fe-bearing minerals). The different thermal behaviour of magnetic extracts and residues versus the bulk sample strongly supports this idea. For the loess sample, the sum of $\chi - T$ curves of the magnetic extract and the residue (Fig. 3b) falls below that of $\chi - T$ curves for the bulk loess sample. Therefore, the susceptibility enhancement of the loess sample on heating must be a result of the matrix-induced reduction (probably caused by small amounts of organic matter, which remains in the non-magnetic residue) of the Fe released from Fe-bearing aeolian particles contained in the extracts. In the mature palaeosols, pedogenesis has largely consumed these aeolian Fe-bearing particles. Therefore, the ratio of $\chi_{\mathrm{ph}}/\chi_{\mathrm{I}}$ is almost 1.

5 CONCLUSIONS

We investigated the temperature dependence of magnetic susceptibilities in Chinese loess/palaeosols. While cooling curves are dominated by SP + SD magnetites produced during heating, the warming curves show complicated patterns, with three distinctive intervals. From room temperature to ∼280 °C, susceptibility gradually increases as a result of the unblocking of fine-grained magnetic particles. Between ∼280–400 °C, the significant decrease of susceptibility is pedogenesis-dependent, resulting from the inversion of fine-grained maghemite to haematite. Above 400 °C, neoformation of SD magnetites begins to occur. Most of the newly formed fine-grained (SP + SD) particles with a dominant grain size around 35 nm are produced above 500 °C.

We found that the final susceptibility after a 700 °C heat treatment is nearly independent of pedogenesis and saturates at ∼33–35 $\times$ 10^{-7} m^3 kg^{-1}. The susceptibility enhancement is caused by the reduction of alteration products of Fe-bearing aeolian minerals (not pedogenic haematite) during heating. It appears that the 700 °C thermal treatment in the argon environment and the pedogenic processes have some equivalent effects on the susceptibility enhancement. Thus, we predict that ∼33–35 $\times$ 10^{-7} m^3 kg^{-1} is the maximum susceptibility that pedogenesis can generate for the S1 unit. The maximum χ_{ph} for the other apparent loess/palaeosol units may be different as a result of potential changes in the aeolian inputs.

ACKNOWLEDGMENTS

We thank B. Carter-Stiglitz for sampling from the YB section. We are grateful to constructive comments by K. L. Verosub and A. J. van Velzen. This study was supported by the National Natural Science Foundation of China (grants 40221402 and 40325011), National Science Foundation (NSF) grant nos EAR 0003421 and EAR/IF 9818704, and the Spanish Ministerio de Ciencia y Tecnología, project AGL2003–01510. CD acknowledges further support from the Royal Society in the form of a BP Amoco Research Fellowship. All rock magnetic measurements were measured at the Institute for Rock Magnetism (IRM), which is supported by the W. M. Keck Foundation, the Earth Science Division of the US National Science Foundation and the University of Minnesota. This is IRM publication 0412.

REFERENCES

Barrón, V. & Torrent, J., 2002. Evidence for a simple pathway to maghemite in Earth and Mars soils, *Geochim. Cosmochim. Acta.,* **66,** 2801–2806.

de Boer, C.B. & Dekkers, M.J., 1996. Grain-size dependence of the rock magnetic properties for a natural maghemite, *Geophys. Res. Lett.,* **23,** 2815–2818.

Chantrell, R.W., El-Hilo, M. & O'Grady, K., 1991. Spin-glass behavior in a fine particle system, *IEEE Trans. Magn.,* **27,** 3570–3578.

Chen, F.H., Bloemendal, J., Feng, Z.D., Wang, J.M., Parker, E. & Guo, Z.T., 1999. East Asian monsoon variations during Oxygen Isotope Stage 5: evidence from the northwestern margin of the Chinese loess plateau, *Quat. Sci. Rev.,* **18,** 1127–1135.

Dankers, P.H.M., 1978. Magnetic properties of dispersed natural iron-oxides of known grain size, *PhD thesis,* University of Utrecht, the Netherlands.

Day, R., Fuller, M.D. & Schmidt, V.A., 1977. Hysteresis properties of titanomagnetites: grain-size and compositional dependence, *Phys. Earth planet. Int.,* **13,** 260–267.

Deng, C.L., Zhu, R.X., Verosub, K.L., Singer, M.J. & Yuan, B.Y., 2000. Paleoclimatic significance of the temperature-dependent susceptibility of Holocene loess along a NW-SE transect in the Chinese loess plateau, *Geophys. Res. Lett.,* **27,** 3715–3718.

Deng, C.L., Zhu, R.X., Jackson, M.J., Verosub, K.L. & Singer, M.J., 2001. Variability of the temperature-dependent susceptibility of the Holocene eolian deposits in the Chinese Loess Plateau: A pedogenesis indicator, *Phys. Chem. Earth, Part A,* **26,** 873–878.

Deng, C.L., Zhu, R.X., Verosub, K.L., Singer, M.J. & Vidic, N.J., 2004. Mineral magnetic properties of loess/paleosol couplets of the central loess plateau of China over the last 1.2 Myr, *J. geophys. Res.,* **109,** B01103, doi:10.1029/2003JB002532.

Eyre, J.K. & Shaw, J., 1994. Magnetic enhancement of Chinese loess – the role of γ Fe_2O_3?, *Geophys. J. Int.,* **117,** 265–271.

Fine, P., Verosub, K.L. & Singer, M.J., 1995. Pedogenic and lithogenic contributions to the magnetic susceptibility record of the Chinese loess/paleosol sequence, *Geophys. J. Int.,* **122,** 97–107.

Florindo, F., Zhu, R.X., Guo, B., Yue, L.P., Pan, Y.X. & Speranza, F., 1999. Magnetic proxy climate results from the Duanjiapo loess section, southernmost extremity of the Chinese loess plateau, *J. geophys. Res.,* **104,** 645–659.

Gallagher, K.J., Feitknecht, W. & Mannweiler, U., 1968. Mechanism of oxidation of magnetite to γ-Fe_2O_3, *Nature,* **217,** 1118–1121.

Gittleman, J.I., Abelas B. & Bozowski, S., 1974. Superparamagnetism and relaxation effects in granular Ni-SiO_2 and Ni-Al_2 O_3 films, *Phys. Rev.,* **B9,** 3891–3897.

Heller, F. & Evans, M.E., 1995. Loess magnetism, *Rev. Geophys.,* **33,** 211–240.

Hrouda, F., 2003. Indices for numerical characterization of the alteration processes of magnetic minerals taking place during investigation of temperature variation of magnetic susceptibility, *Stud. Geophys. Geodaet.,* **47,** 847–861.

Hrouda, F., Müller, P. & Hanák, J., 2003. Repeated progressive heating in susceptibility vs. temperature investigation: a new paleotemperature indicator? *Phys. Chem. Earth,* **28,** 653–657.

Ji, J.F., Balsam, W., Chen, J. & Liu, L.W., 2002. Rapid and quantitative measurement of hematite and goethite in the Chinese loess-paleosol sequence by diffuse reflectance spectroscopy, *Clays Clay Miner.,* **50,** 208–216.

Ji, J.F., Balsam, W., Lu, H.Y., Sun, Y.B. & Xu, H.F., 2004. High resolution hematite/goethite records from Chinese loess sequences for the last glacial-interglacial cycle: Rapid climatic response of the East Asian Monsoon to the tropical Pacific, *Geophys. Res. Lett.,* **31,** L03207, doi:10.1029/2003GL018975.

Khater, A., Ferre, J. & Meyar P., 1987. Spin-cluster theory in magnetic materials and applications to a spin glasses, *J. Phys. C: Solid State Phys.,* **20,** 1857.

Liu, Q.S., Banerjee, S.K., Pan, Y.X. & Zhu, R.X., 2002. Effects of low-temperature oxidation on the natural remanent magnetization carried by the Chinese loess, *Chin. Sci. Bull.,* **47,** 2100–2105.

Liu, Q.S., Banerjee, S.K., Jackson, M.J., Chen, F.H., Pan, Y.X. & Zhu, R.X., 2003. An integrated study of the grain-size dependent magnetic mineralogy of the Chinese loess/paleosol and its environmental significance, *J. geophys. Res.,* **108,** 2437, doi:10.1029/2002JB002264.

Liu, Q.S., Banerjee, S.K., Jackson, M.J., Chen, F.H., Pan, Y.X. & Zhu, R.X., 2004a. Determining the climatic boundary between the Chinese loess and palaeosol: evidence from aeolian coarse-grained magnetite, *Geophys. J. Int.,* **156,** 267–274.

Liu, Q.S., 2004b, Pedogenesis and its effects on the natural remanent magnetization acquisition history of the Chinese loess, Ph.D. thesis.

Liu, Q.S., Banerjee, S.K., Jackson, M.J., Maher, B.A., Pan, Y.X., Zhu, R.X., Deng, C.L. & Chen, F.H., 2004c. Grain sizes of susceptibility and anhysteretic remanent magnetization carriers in Chinese loess/paleosol sequences, *J. Geophys. Res.,* **109,** B03101, doi:10.1029/2003JB002747.

Liu, Q.S., Jackson, M.J., Yu, Y., Chen, F.H., Deng, C.L. & Zhu, R.X., 2004d. Grain size distribution of pedogenic magnetic particles in Chinese loess/paleosols, *Geophys. Res. Lett.,* **31,** L22603, doi:10.1029/2004GL021090.

Liu, T.S., 1985. *Loess and the Environment,*, China Ocean Press, Beijing, p. 251.

Maher, B.A., 1988. Magnetic properties of some synthetic sub-micron magnetites, *Geophys. J.,* **94,** 83–96.

Maher, B.A., 1998. Magnetic properties of modern soils and Quaternary loessic paleosols: paleoclimatic implications, *Palaeogeog., Palaeoclimat., Palaeoecol.,* **137,** 25–54.

Maher, B.A. & Thompson, R., 1991. Mineral magnetic record of the Chinese loess and paleosol, *Geology,* **19,** 3–6.

Maher, B.A. & Thompson, R., 1992. Paleoclimatic significance of the mineral magnetic record of the Chinese loess and paleosols, *Quat. Res.,* **37,** 155–170.

Mullender, T.A.T., van Velzen, A.J. & Dekkers, M.J., 1993. Continuous drift correction and separate identification of ferrimagnetic and paramagnetic contributions in thermomagnetic runs, *Geophys. J. Int.,* **114,** 663–672.

Oches, E.A. & Banerjee, S.K., 1996. Rock-magnetic proxies of climate change from loess-paleosol sediments of the Czech Republic, *Stud. Geophys. Geodaet.,* **40,** 287–300.

Özdemir, Ö., 1990. High-temperature hysteresis and thermoremanence of single-domain maghemite, *Phys. Earth planet. Int.,* **65,** 125–136.

Özdemir, Ö. & Banerjee, S.K., 1982. A preliminary magnetic study of soil samples from west-central Minnesota, *Earth planet. Sci. Lett.,* **59,** 393–403.

Porter, S.C., Hallet, B., Wu, X.H. & An, Z.S., 2001. Dependence of near-surface magnetic susceptibility on dust accumulation rate and precipitation on the Chinese Loess Plateau, *Quat. Res.,* **55,** 271–283.

Schwertmann, U. & Taylor, R.M., 1989. Iron oxides, in, *Minerals in Soil Environments,* 2nd edn, pp. 379–438, eds Dixon, J.B. & Weed, S.B., Soil Science Society of America, Madison, WI.

Senno, H., Tawara, Y. & Iida, Y., 1967. Transformation of γ-Fe_2O_3 into α-Fe_2O_3, *Jap. J. App. Phys.,* **6,** 1347–1348.

Sun, J.M., 2002. Provenance of loess material and formation of loess deposits on the Chinese Loess Plateau, *Earth planet. Sci. Lett.,* **203,** 845–859.

Sun, W.W., Banerjee, S.K. & Hunt, C.P., 1995. The role of maghemite in the enhancement of magnetic signal in the Chinese loess-paleosol sequence: An extensive rock magnetic study combined with citrate-bicarbonate-dithionite treatment, *Earth planet. Sci. Lett.,* **133,** 493–505.

Tite, M.S., 1975. Effect of climate on the magnetic susceptibility of soils, *Nature,* **256,** 565–566.

van Velzen, A.J. & Dekkers, M.J., 1999. The incorporation of thermal methods in mineral magnetism of loess-paleosol sequences: a brief overview, *Chinese Sci. Bull.,* **44,** (Supp. 1), 53–63.

Verosub, K.L., Fine, P., Singer, M.J. & TenPas, J., 1993. Pedogenesis and paleoclimate: Interpretation of the magnetic susceptibility record of Chinese loess-paleosol sequences, *Geology,* **21,** 1011–1014.

Verwey, E.J., Haayman, P.W. & Romeijn, F.C., 1947. Physical properties and cation arrangement of oxides with spinel structures, *J. Chem. Phys.,* **15,** 181–189.

Vidic, N.J., TenPas, J.D., Verosub, K.L. & Singer, M.J., 2000. Separation of pedogenic and lithogenic components of magnetic susceptibility in the Chinese loess/paleosol sequence as determined by the CBD procedure and a mixing analysis, *Geophys. J. Int.,* **142,** 551–562.

Zhou, L.P., Oldfield, F., Wintle, A.G., Robinson, S.G. & Wang, J.T., 1990. Partly pedogenic origin of magnetic variations in Chinese loess, *Nature,* **346,** 737–739.

Zhu, R.X., Lin, M. & Pan, Y.X., 1999. History of the temperature-dependence of susceptibility and its implications: Preliminary results along an E–W transect of the Chinese Loess Plateau, *Chin. Sci. Bull.,* **44,** supplement 1,81–86.

Zhu, R.X., Matasova, G., Kazansky, A., Zykina, V. & Sun, J.M., 2003. Rock magnetic record of the last glacial-interglacial cycle from the Kurtak loess section, southern Siberia, *Geophys. J. Int.,* **152,** 335–343.

Zhu, R.X., Liu, Q.S. & Jackson, M.J., 2004. Paleoenvironmental significance of the magnetic fabrics in Chinese loess-paleosols since the last interglacial (<130 ka)., *Earth planet. Sci. Lett.,* **221,** 55–69.